

Design Space Exploration of Next-Generation Supersonic Business Jet Engine with a Focus on Landing and Take-off (LTO) Noise

Dario Del Gatto^{1*}, Stylianos Adamidis¹, Christos Mourouzidis¹, Stephen Brown¹, Vassilios Pachidis¹

1. Centre for Propulsion and Thermal Power Engineering, Cranfield University, MK43 0AL, United Kingdom

Abstract

The present paper illustrates the engine design space exploration for a Mach 1.6 – 10 pax supersonic business jet, to assess the impact of the Landing and Take-off (LTO) noise constraint on the engine cycle design. A reference exhaust jet Mach number of 0.95 was selected as representative noise limit at the take-off phase of civil supersonic powerplants. A two-spool mixed-flow turbofan engine with fixed throat and variable exit area convergent-divergent nozzle is considered as the baseline for this study (MFTF). The noise limitation impact on this architecture cycle design is highlighted herein. This results in a relatively low specific net thrust. An additional variability is considered via a fully variable throat and exit area nozzle (MFTF-VA) to meet the noise related requirement with higher specific net thrust engines. For both architectures, limitations and potential benefits in terms of cycle efficiency and engine size are illustrated. Although fan operability limits the available design space, the MFTF-VA allows for a 24% increase in specific net thrust compared to the MFTF. This corresponds to 8% and 15% decrease in fan size and engine weight, for the specified noise limit.

Keywords: supersonic, business-jet, noise, turbofan, LTO.

1. Introduction

In the last decades, several projects were launched to investigate civil supersonic flight [1], [2], [3] and the endeavors of several industry players have brought the world back to the verge of the next supersonic transport era [4]. In this context of renewed interest for supersonic flight, the ICAO and the EU aim to understand the environmental impact of these vehicles in order to establish relevant regulations and certification processes. Since current data only pertains to the Concorde era, comprehensive studies are essential. Thus, the EU funded the SENECA Project [5] ("LTO Noise and Emissions of Supersonic Aircraft"), in which the present work falls, has been launched to support this research.

Engine cycle design for supersonic engines is constrained by numerous requirements. As their subsonic counterparts, they need to satisfy the aircraft requirements at all flight conditions. Most importantly, building from the Concorde's and Tupolev's experience, they need to be not only fuel efficient but also to be compliant with todays and future aviation emissions goals for supersonic aircraft to be perceived as viable.

Emissions constraints regard both pollutant and noise emissions. Noise is particularly important during supersonic flight (sonic boom) and in the airport vicinity (Landing and Take-off cycle, LTO).

The preferred choice for civil supersonic engine architectures is a mixed flow turbofan. Initial feasibility studies were proposing very-low bypass ratio (BPR <1) [6] turbofan engines that offer higher specific net thrust during supersonic operations but require additional noise abatement features for noise requirements. Current studies look at higher BPRs (~1.5-3) [7], [8] due to the best performance for LTO noise.

Available studies in the literature investigate mixed flow engines with a fixed throat area nozzle [9].In

the N+2 study [3] NASA illustrates the design process for a 30 Pax and 100Pax supersonic business jet and airliner respectively. In the design process, it is stated that the nozzle throat area is varied to maintain sufficient margin from surge for the fan. Part-power operations are then performed considering a fixed throat area equal to the one previously calculated.

The present work investigates the impact of a fully variable (throat and exit) area nozzle on the engine design for a Mach 1.6 supersonic business jet, the Cranfield "Aeolus" E-19 [10], and assess its performance and operability particularly during take-off. Although as previously mentioned, supersonic aircraft will face noise-related limitations both at high altitude supersonic operations and during the LTO cycle, for this study it is assumed that the aircraft will fly supersonic only "over-water" and subsonic "over-land", hence high-altitude operation limitations related to 'sonic boom' fall out of the research scope. Moreover, although the SENECA project addresses the LTO cycle, for the present work the take-off part is the focus of the analysis.

2. Engine Design Methodology

The E-19 is a 10-passenger aircraft designed for a flight range of 4000 nmi with a M1.6 cruise speed. Six main flight segments, namely take-off, subsonic climb, transonic acceleration, supersonic climb, supersonic cruise, and descent characterize the baseline mission profile. The aircraft performs a rapid initial climb to reach the 10000 m mark avoiding subsonic traffic and then performs a transonic acceleration from Mach 0.95 to 1.3. Subsequently, it climbs supersonically reaching Mach 1.6 and then it climb-cruises with a constant Mach number [11].

For this study, a two-spool mixed-flow turbofan engine architecture has been selected. The engine design was assessed with a fixed throat and variable exit area nozzle (MFTF), as well as with a fully variable throat and exit area nozzle (MFTF - VA). The engine performance model block diagram is illustrated in Figure 1. Black lines represent the mechanical power connections. The auxiliary power (AuxPwr) is assumed to be extracted from the high-pressure spool. The blue arrow lines represent flow connections with direction. For both turbines, cooling flow calculations are performed for both NGVs and Rotors at the supersonic cruise point, while the additional cooling (~1% of the incoming high pressure compressor flow (HPCfow)) is considered for disk cooling and purging [12].

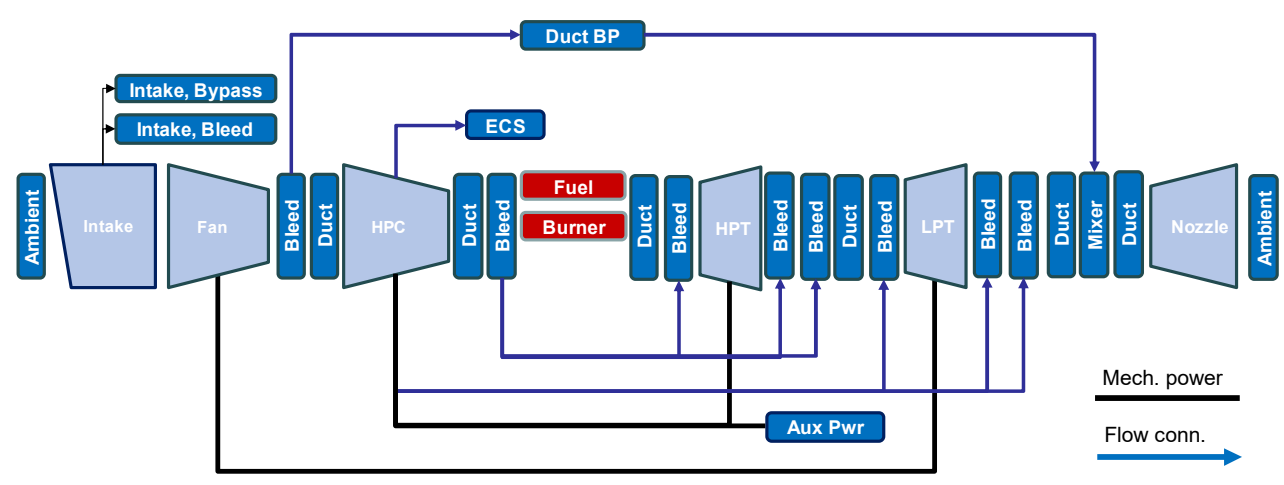


Figure 1 – Engine block diagram.

Engine technology levels are based on public domain data for a 2025-2035 entry-into-service [3], [6], [13]. After engine-lifing considerations, a maximum high-altitude operating temperature limit of 850K, 1750K and 1650K and a maximum take-off operating temperature limit of 950K, 1950K and 1850K have been selected for the compressor delivery (T30), turbine NGV inlet (T40) and turbine rotor inlet temperature (T41), respectively. Turbine blade metal temperature limit for continuous operation reflect those of nickel-based superalloy blades. These are set to 1170K and 1070K for the high-pressure turbine (HPT) and low-pressure turbine (LPT), respectively. For the mixer at design point, a unitary extraction ratio (ER) is assumed, while a 0.85 mixing efficiency (η_{comb}) is considered along with a 0.45 mixer outlet Mach number (M_{64}). Combustion efficiency (η_{comb}) is set to 0.9999. A limit on the exhaust jet Mach number ($M_{noz,ex}$) at take-off is set to 0.95, to allow the engine to be compliant with the noise

constraint, while avoiding any shock generation on the nozzle walls. Fan and High-pressure compressor (HPC) polytropic efficiencies, with HPT and LPT isentropic efficiencies are shown in Table 1 below, which provides a complete overview of the engine design limits and inputs.

Table 1 – Technology assumptions

	Techno	logy Assumptions					
Efficiencies η _{@DP}		Duct Pressure Losses					
Fan η _{pol}	0.90	Swan Neck	1.0%				
HPC η _{pol}	0.91	Combustor	4.7%				
η _{comb}	0.9999	LPT Turbine Exit Duct	1.0%				
HPT η _{is}	0.91	Bypass Duct	2.0%				
LPT η _{is}	0.92	Tailpipe	0.5%				
Core Temperature Limitations [K]							
SMCr HPT blade	1170	High alt. T41 max	1650				
SMCr LPT blade	1070	MTO T30 max	950				
High alt. T30 max	850	MTO T40 max	1950				
High alt. T40 max	1750	MTO T41 max	1850				
Exhaust Jet Noise Limitation for Take-off							
$\mathbf{M}_{noz,\epsilon}$	M _{noz,ex}		0.95				
Mixer Inputs							
Mixer η _{mix}	0.85	Mixer ER	1.0				
Mixer M ₆₄	0.45						
Bleed Take-off							
ECS	~1% HPC _{flow}	Disc cooling	~1% HPC _{flow}				

The engine installed performance is assessed within an integrated framework that combines the Numerical Propulsion System Simulation (NPSS), an advanced object-oriented, non-linear thermodynamic modelling environment [14], [15], and the Performance of Installed Propulsion Systems Interactive (PIPSI) methodology [16], that accounts for the installation effects of the supersonic intake and exhaust systems. For the engine cycle design in NPSS, a multi-point design approach is used. This involves five engine key operating points, namely the supersonic mid-cruise (SMCr), supersonic top of climb (STOC), end and beginning of transonic acceleration (ETR and BTR) and maximum take-off (MTO). An iteration loop ensures that the thrust requirements are met while all design constraints are respected. Table 2 offers a summary of the main thrust requirements for the engine cycle design, while a visual representation of the multi-point design iteration loop is illustrated in Figure 2.

Table 2 - Engine cycle design points

Operating point	Altitude [m]	Flight M [-]	Thrust [kN]	
SMCr	16277	1.6	18.2	
STOC	14804	1.6	25.8	
ETR	10000	1.3	38.3	
BTR	10000	0.95	27.6	
MTO	10	0.3	67.9	

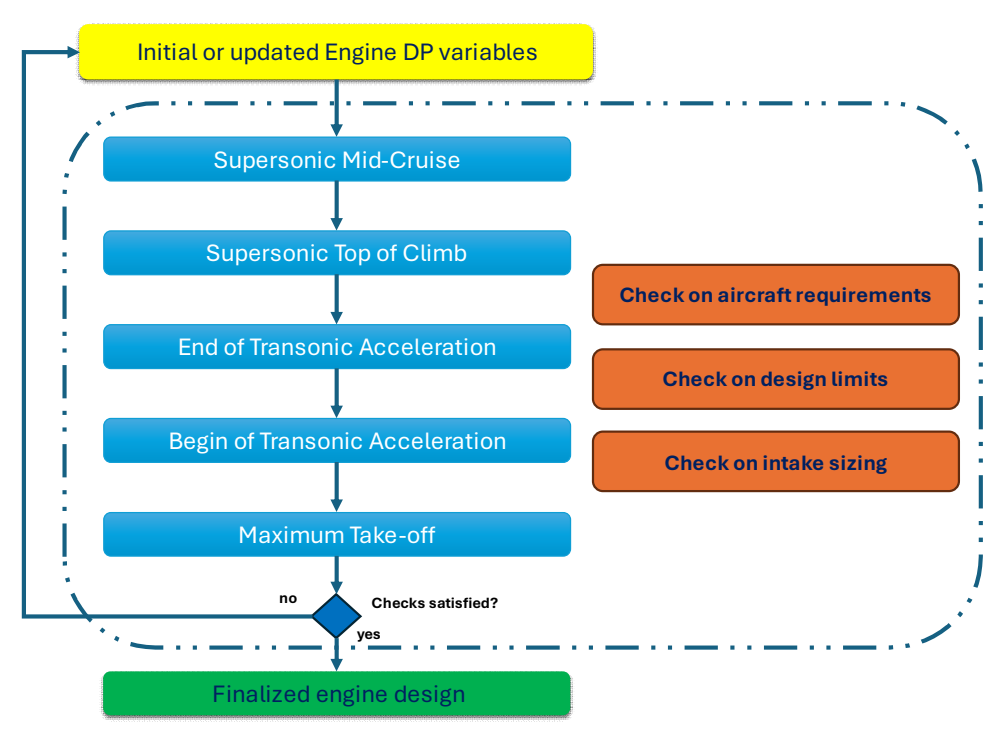


Figure 2 – Multi-point design approach.

The PIPSI methodology summarizes the intake components behavior into performance maps. These maps are collected from NASA's theoretical studies and experimental test campaigns. For the intake, this methodology allows the accounting for throttle-dependent forces, total pressure recovery, shock stability, and boundary layer-shock interaction bleed requirements [16].

A new NPSS intake element has been developed following this methodology. In this element, the calculations are performed as illustrated in Figure 3. For each operating point in the cycle design loop, the intake element calculates the different drag coefficients (Cds) and the intake pressure recovery (P rec). Additionally, an internal routine calculates the "ideal" capture area, that estimates the intake capture area required at each point if they were to be considered as the intake sizing point, operating on critical condition. An initial guess on the intake capture area is then iterated by the solver up until it matches the maximum ideal capture area calculated across the design points.

For the afterbody drag, an assumption is made on the nacelle maximum cross-sectional area. This section is assumed to be squared and its side is assumed to be 5% larger than the fan diameter. Based on this and on the reference afterbody drag map, the relative afterbody drag coefficient is calculated for each operating condition.

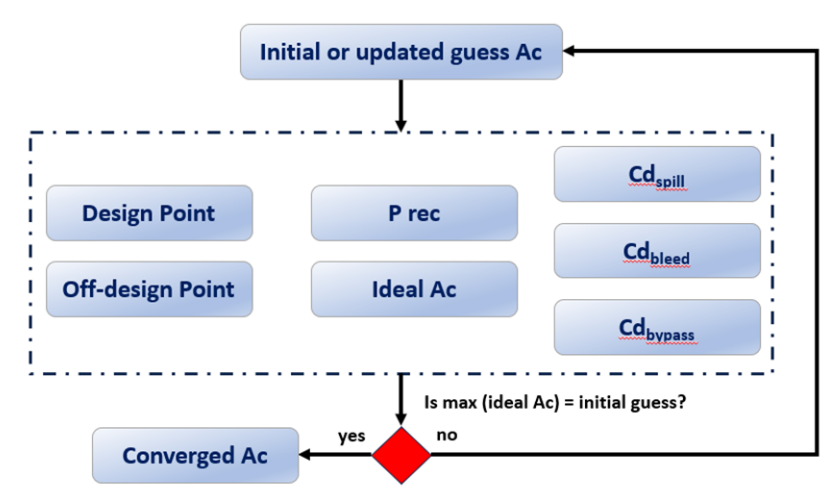


Figure 3 – Intake element flowchart.

3. Results

Figure 4 illustrates the engine preliminary design space exploration assuming a MFTF configuration in terms of specific fuel consumption (SFC) at SMCr, fan diameter and nozzle throat Mach number at MTO. The SFC curve follows a parabolic trend, reaching a minimum (~30.4 g/kN/s) between 200 and 220 N/kg/s of SMCr specific net thrust (SpFn). The fan diameter is calculated for the maximum capacity design point. This occurs at the transonic acceleration for the whole range of SMCr SpFn shown here. The fan size reduces progressively from 1.55 to 0.9 m at the SpFn range extremes. The MTO nozzle exhaust M is subsonic for the lower end of the SpFn range. For SpFn higher than 210 N/kg/s, the nozzle is choked at this operating condition.

Appling the limitation on noise at MTO, it is clear how this stringent limit confines the engine design space severely. For the selected aircraft, the design is limited to a maximum SMCr SpFn of 186 N/kg/s, hence to a fan size of 1.35 m.

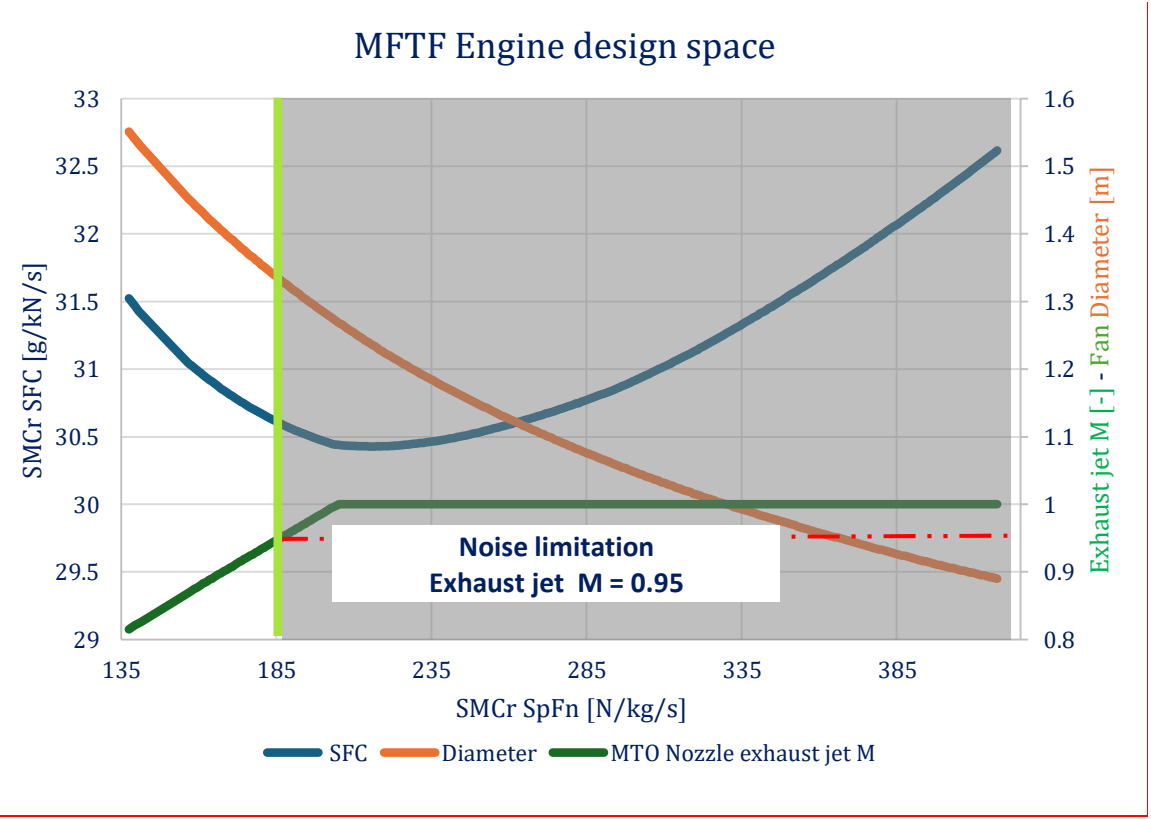


Figure 4 - Engine design space (SFC, Fan diameter, Exhaust jet M vs SpFn)

Aircraft mission performance and fuel burn is a combination of several parameters including the engine performance, size, and weight. Especially for the case of supersonic vehicles, drag related elements present a significantly stronger impact on fuel efficiency than engine efficiency. For this reason, aiming for higher SpFn cycles than the one achieved with a MFTF is necessary.

To overcome the limitation imposed by the noise limit at take-off, an additional variability is considered on the nozzle design, assuming a fully variable throat and exit areas (MFTF-VA). Increasing the nozzle throat area allows the NPR to be reduced. On one hand this causes the engine mass flow to increase compensating the reduced flow kinetic power. For a fixed MTO net thrust, this allows the MTO SpFn to decrease for the same SMCr SpFn. This area variability is introduced via a solver pair in the cycle design algorithm to meet the required exhaust jet Mach number by varying the nozzle throat area. For this configuration, the engine behaviour is dictated by the required nozzle critical pressure ratio which sets the required engine mass flow for this condition. For the same noise limitation at take-off, applying the variable area configuration increases the cycle SMCr SpFn by ~24%, corresponding to an overall 8% diameter and ~0.6% SFC reduction, respectively, as shown in Figure 5.

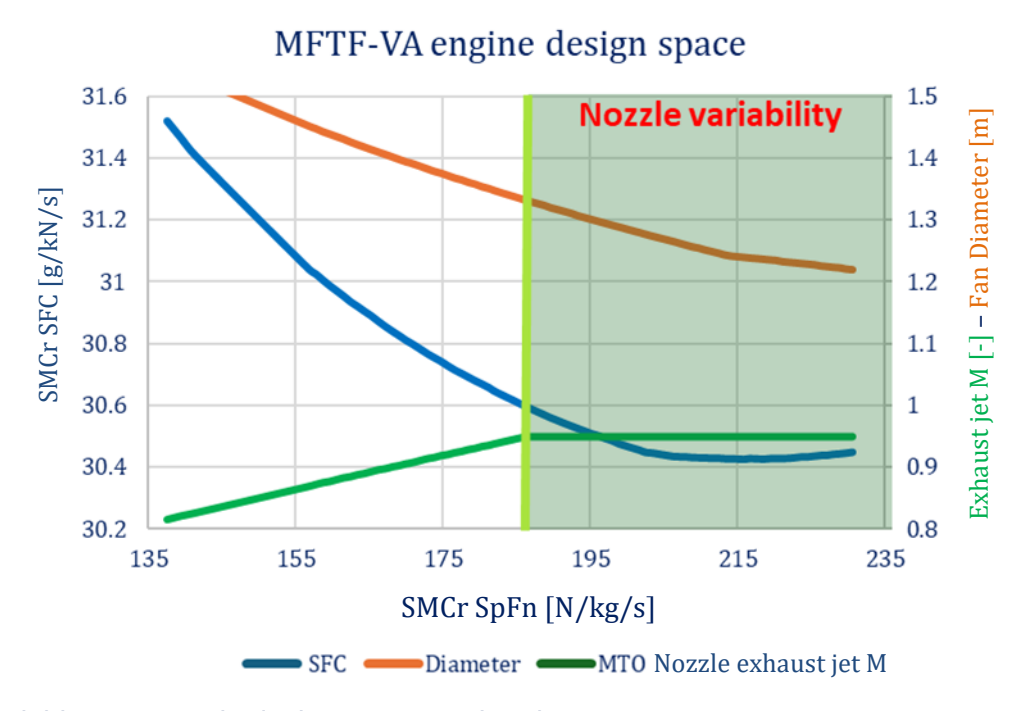


Figure 5 - Variable area nozzle design space exploration.

This variability affects the engine operability, specifically in terms of the fan operating line. Figure 6a) shows the fan characteristics for SMCr SpFn 186, 207 and 230 N/kg/s to compare the fan operating point for all the cycles in the same plot. Setting a target on nozzle exit M (thus NPR) at MTO, determines the fan pressure ratio at MTO. Consequently, as the design fan pressure ratio progressively increases with SpFn, the MTO operating points on the fan characteristics progressively move towards the chocking region of the map. Although this might be related to the actual map used, it is noted that operating in this low fan efficiency region might lead to mechanical issues.

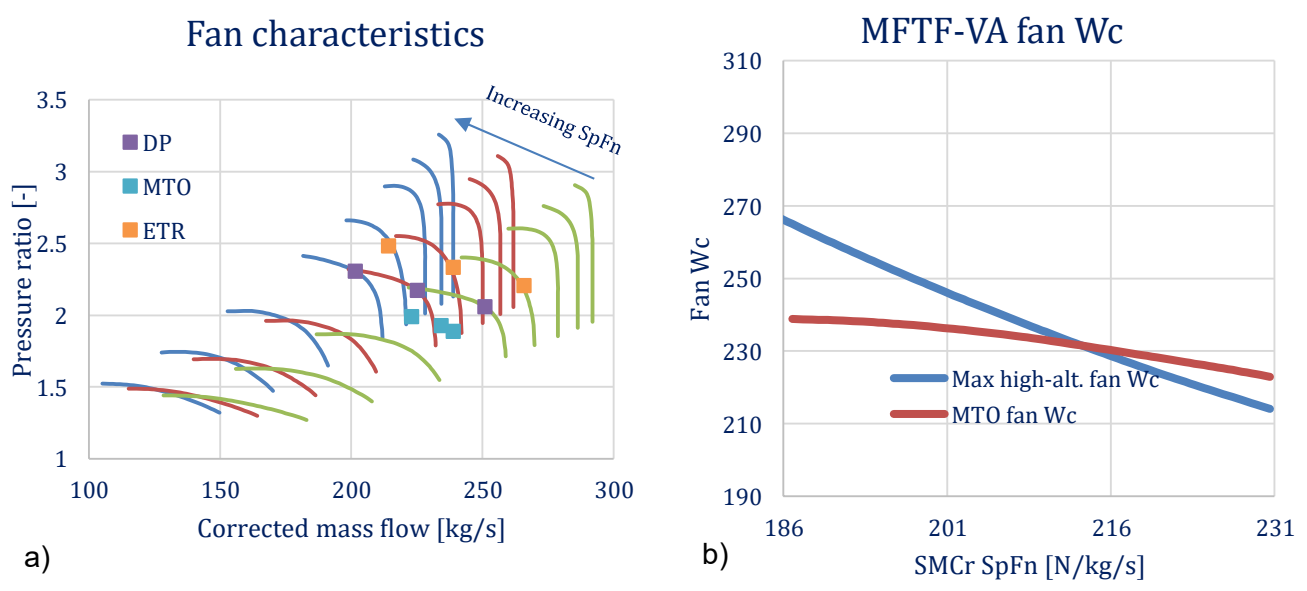


Figure 6 – a) Fan characteristic and MTO operating points b) MTO and ETR Wc comparison

Furthermore, for engine designs with SMCr SpFn values greater than 214 N/kg/s, the fan corrected mass flow (Wc) at MTO surpasses that of the ETR, as it can be seen in Figure 6b. This means that for the higher specific thrust region of the design space, the fan capacity is no longer maximum at ETR but at MTO conditions. Thus, there is a need change the fan sizing point from the ETR to the MTO for SMCr SpFn higher than 214 N/kg/s, hence the kink in the fan diameter curve in Figure 5.

Figure 7 illustrates the impact of adopting nozzle variability on the engine core temperatures. Across the entire SMCr SpFn range, the most demanding point is the STOC, where the limits on T30 and T41 are reached. In contrast, the MTO core temperatures remain well below the prescribed limits for this condition. During MTO, the fan operates in an unfavorable efficiency region of its characteristics, leading to an increase in HPC delivery temperature.

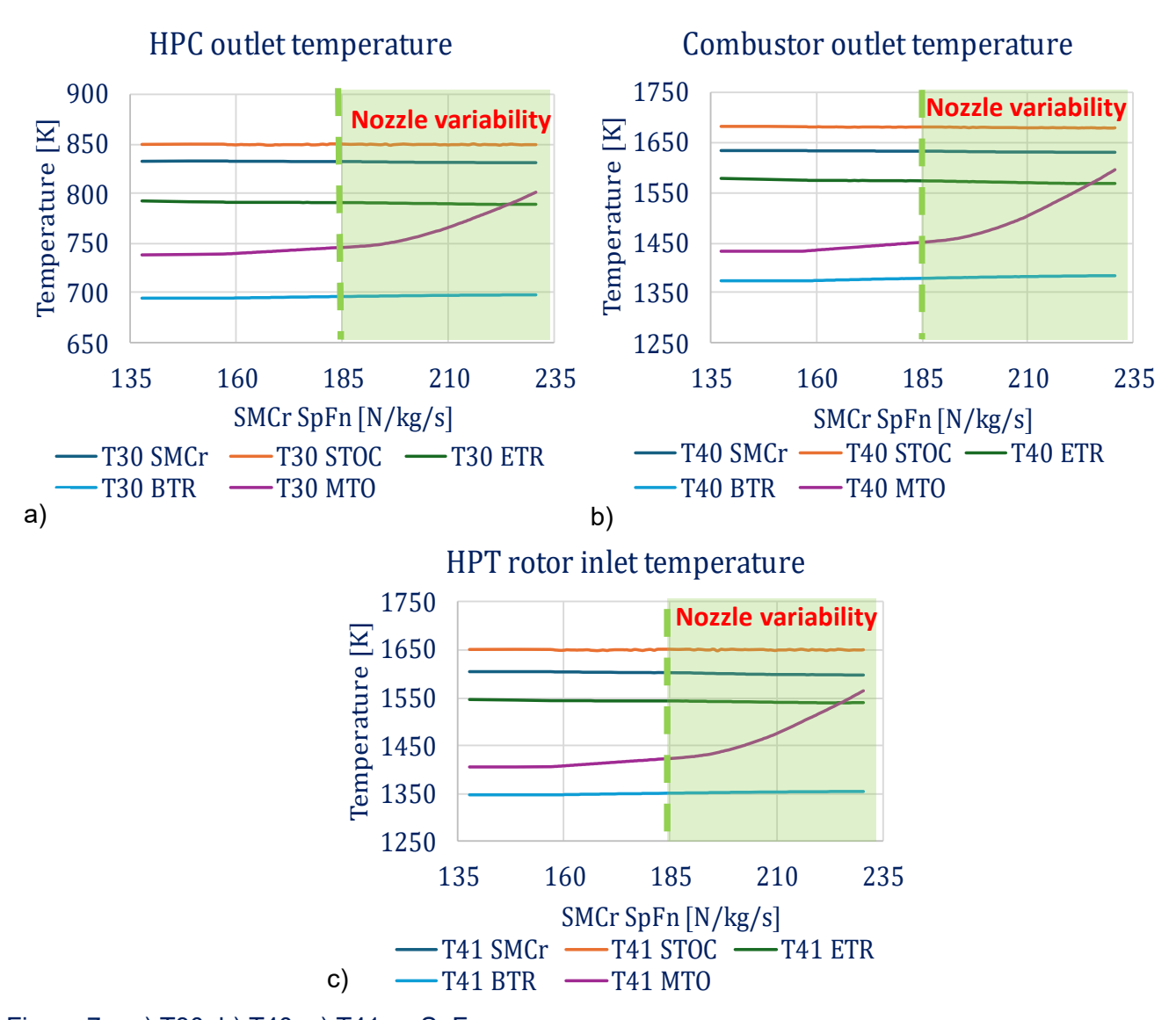


Figure 7 – a) T30, b) T40, c) T41 vs SpFn.

Similarly, T40 and T41 at MTO tend to rise with increasing SMCr SpFn. This can be understood by examining Figure 8. As SMCr SpFn increases, the MTO BPR slope becomes less steep after 186 N/kg/s. This is due to the need for increased bypass mass flow to reduce the jet kinetic power. In turn the fan's inlet mass flow (W2) and required work increases. This loss in fan outlet pressure and the increased fan outlet temperature lead to an increased core net power output (especially for LPT), as shown in Figure 9b. Since the core mass flow (W24) remains constant, this results in a progressive increase in combustor delivery temperature, hence fuel flow (Wff).

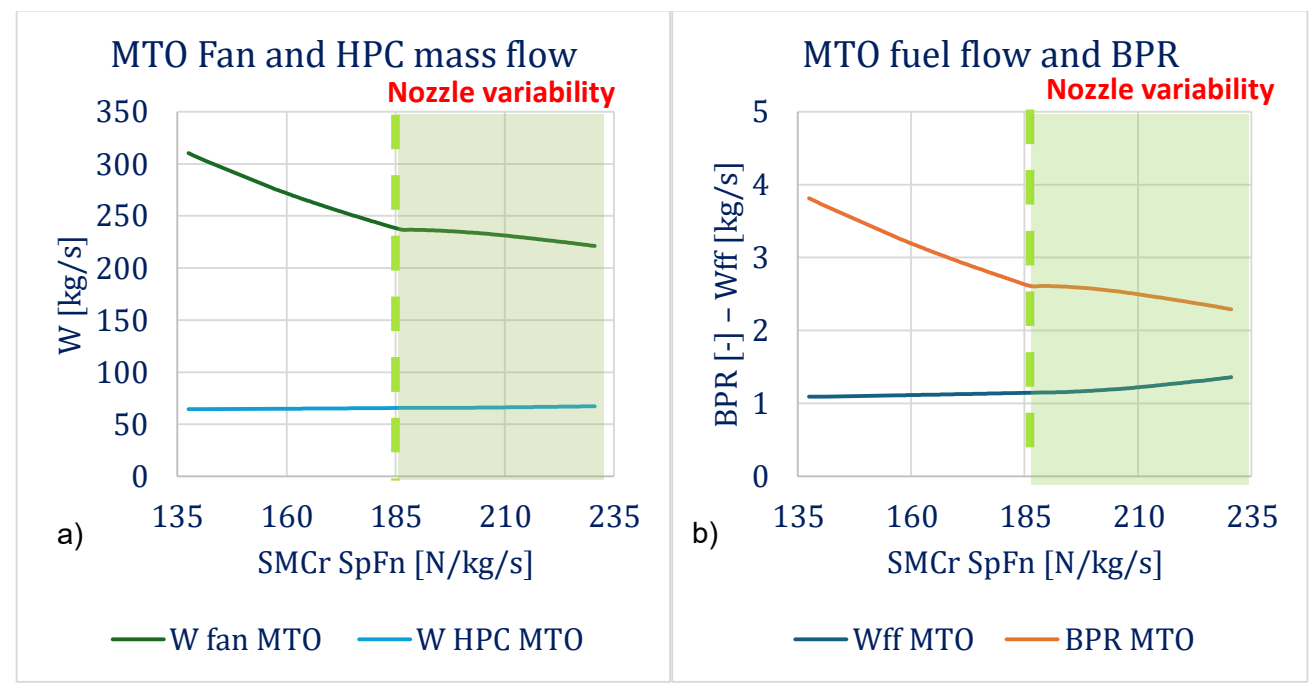


Figure 8 – a) BPR and Wf vs SMCr SpFn b) Fan and HPC inlet mass flow.

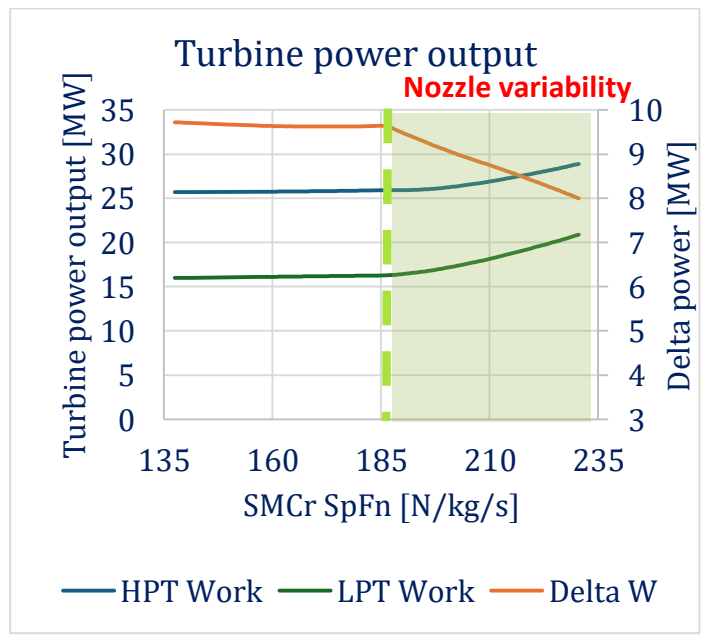


Figure 9 – Turbine power output.

Figure 10 shows the engine preliminary weight assessment. The bare engine weight is calculated using Cranfield's ATLAS [17] while for the supersonic intake system empirical relationships are included [16]. The exhaust nozzle is assumed to be 33% of the bare engine weight [18] . The additional features (actuators, hinges, etc.) for a fully variable area nozzle are deemed to have a secondary effect on the powerplant overall weight.

The overall engine weight tends to decrease as the SMCr SpFn increases. The kink point at 214 N/kg/s is related to the aforementioned fan size trend. The green line highlights the overall engine weight for the MFTF engine design with SMCr SpFn of 186 N/kg/s. The overall weight of this powerplant is 3850 kg. In the case of MFTF-VA engine design with SMCr SpFn of 230 N/kg/s, given the increased SpFn, the overall weight per engine is reduced by 15% to 3250 kg. Since the E-19 has a twinjet engine configuration, this leads to a global 1200 kg total engine weight reduction. This does not include the impact of the nacelle weight reduction due to the smaller engine cross-sectional size, which assessment is out of the scope of this work.

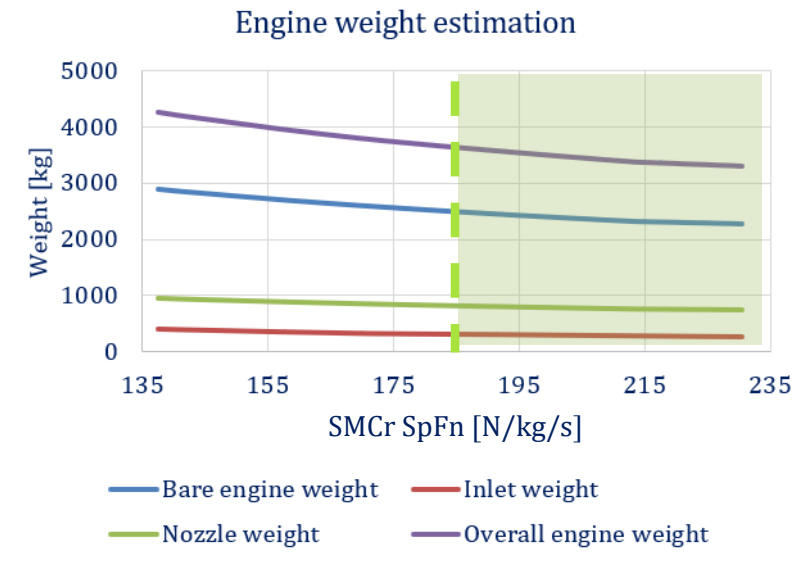


Figure 10 - Engine weight assessment.

The final cycle selected for the E-19 aircraft is that with the maximum SpFn available for the MFTF-VA engine configuration. Table 3 provides the key operating parameters for this cycle, while Figure 11 shows the engine annulus diagram. The selected engine design includes a 2-stage fan with a 1.22m fan diameter and a 7-stage HPC. The HPT is configured as a single stage, while the LPT employs a 3-stage configuration, accounting noise related considerations.

Table 3 - Selected engine key cycle parameters.

Parameter	SMCr	STOC	ETR	BTR	МТО
FPR [-]	2.305	2.433	2.479	2.422	1.987
OPR [-]	21.2	22.9	23.7	23.1	20.1
BPR [-]	1.74	1.67	1.67	1.71	2.29
T30 [K]	830.8	850.0	788.7	697.6	800.5
T40 [K]	1629.0	1682.5	1568.5	1382.7	1597.3
T41 [K]	1597.8	1650.0	1537.9	1355.6	1566.1

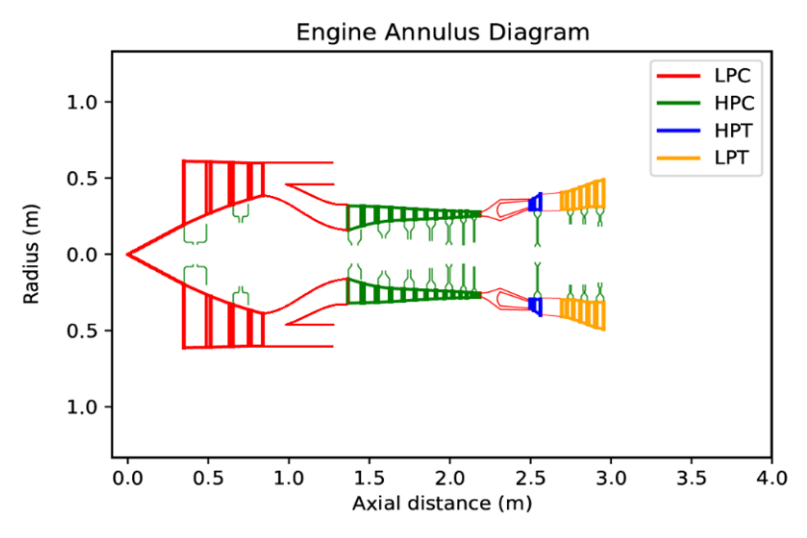


Figure 11 Engine annulus diagram.

3. Conclusions

This paper explores the design space of a supersonic powerplant suitable for a Mach 1.6, 10-passenger supersonic business jet. The engine cycle design employs a 5-design point approach, covering key operating points within the mission envelope. To better represent engine behavior at supersonic speeds, the NASA PIPSI methodology is utilized to evaluate intake and afterbody conditions along with associated drags.

A fixed throat area nozzle arrangement (MFTF engine configuration), constrained by noise limits for the LTO cycle, significantly restricts the engine design space to relatively low Specific Thrust (SpFn) values. For the MFTF engine design with the highest available SpFn, the engine diameter was found to be 1.35 m, with an SFC of 30.6 g/kN/s. However, allowing the nozzle throat to vary at MTO (MFTF-VA engine configuration) increases the available engine design SpFn by 24%. This corresponds to an 8% reduction in fan diameter and a 0.6% reduction in SFC (1.22m and 30.4 g/kN/s respectively). The weight assessment within the design space indicates that this adjustment leads to an overall weight reduction of 15%. For engines with increased SpFn in flight, the required NPR at MTO correlates with an increased non-dimensional mass flow of the fan relative to a fixed area nozzle, and relative to design point and ETR and thus fan operability challenges. This is associated with higher T30, T40 and T41 temperatures at MTO. Thus, it is apparent that the extra degree of freedom provided by the nozzle throat variability can provide an engine design solution with significantly higher SpFn. Considering the aircraft overall performance, the MFTF-VA engine design with the smallest fan diameter and the highest specific thrust available is selected as the most suitable candidate for this application.

4. Contact Author Email Address

dario.del-gatto@cranfield.ac.uk

5. Copyright Statement

The authors confirm that they, and/or their company or organization, hold copyright on all of the original material included in this paper. The authors also confirm that they have obtained permission, from the copyright holder of any third party material included in this paper, to publish it as part of their paper. The authors confirm that they give permission, or have obtained permission from the copyright holder of this paper, for the publication and distribution of this paper as part of the ICAS proceedings or as individual off-prints from the proceedings.

References

- [1] S. Hoffman and S. Hoffman, "Bibliography of Supersonic Cruise Research (SCR) Program From 1977 to Mid-1980 NASA Reference Publication 1063 Bibliography of Supersonic Cruise Research (SCR) Program From 1977 to Mid-1980," 2020.
- [2] J. s. Westmoreland and A. M. Stern, "VARIABLE CYCLE ENGINE TECHNOLOGY PROGRAM," 1978.
- [3] H. R. Wedge *et al.*, "(Boeing N+2) Supersonic Concept Development and Systems Integration," *Nasa Cr*, no. August, p. 216842, 2010.
- [4] B. Supersonic, "Boom Supersonic," 2021.
- [5] DLR, "SENECA (LTO) noiSe and EmissioNs of supErsoniC Aircraft," Https://Seneca-Project.Eu/. [Online]. Available: https://seneca-project.eu/
- [6] J. BERTON and W. HALLER, "A Comparative Propulsion System Analysis for the High-Speed Civil Transport," ..., First Annual High-Speed ..., no. February, pp. 831–866, 1992, [Online]. Available: http://www.csa.com/partners/viewrecord.php?requester=gs&collection=TRD&recid=N9433477AH
- [7] T. R. Conners and D. C. Howe, "Propulsion System Integration and Vehicle Performance," no. January, pp. 1–16, 2005.
- [8] J. J. Berton, S. M. Jones, J. A. Seidel, and D. L. Huff, "Noise predictions for a supersonic business jet using advanced take-off procedures," *Aeronautical Journal*, vol. 122, no. 1250, pp. 556–571, 2018, doi: 10.1017/aer.2018.6.
- [9] T. Schlette and S. Staudacher, "Engine Design Requirements for Supersonic Business Jets," *European Conference on Turbomachinery Fluid Dynamics and Thermodynamics, ETC*, 2021, doi: 10.29008/etc2021-526.
- [10] H. Smith, Y. Sun, and M. Frame, "Design case of the e-19 aeolus supersonic business jet," *Aiaa Aviation 2020 Forum*, 2020, doi: 10.2514/6.2020-2618.

DESIGN SPACE EXPLORATION OF NEXT-GEN. SUPERS. BIZJET ENGINE WITH A FOCUS ON LTO NOISE

- [11] C. Mourouzidis, D. Del Gatto, S. Adamidis, C. V. Munoz, and C. Lawson, "Preliminary design of next generation Mach 1 . 6 supersonic business jets to investigate landing & take-off (LTO) noise and emissions SENECA .," pp. 2–9, 1921.
- [12] P. P. Walsh and P. Fletcher, *Gas turbine performance*. Blackwell Science, 2005.
- [13] J. D. Mattingly, Elements of Propulsion: Gas Turbines and Rockets. 2006. doi: 10.2514/4.861789.
- [14] E. S. Hendricks, "A multi-level multi-design point approach for gas turbine cycle and turbine conceptual design," no. May, 2017.
- [15] T. L. Benyo, "Flow matching results of an MHD energy bypass system on a supersonic turbojet engine using the Numerical Propulsion System Simulation (NPSS) environment," *42nd AIAA Plasmadynamics and Lasers Conference*, no. August 2011, 2011, doi: 10.2514/6.2011-3591.
- [16] E. J. Kowalski, "Computer code for estimating installed performance of aircraft gas turbine engines. Volume 1: Final report," Seattle, WA, USA, 1979. [Online]. Available: https://ntrs.nasa.gov/citations/19800004788
- [17] P. Lolis, "Development of a Preliminary Weight Estimation Method for Advanced Turbofan Engines," *Cranfield University, PhD Thesis*, no. July, p. 214, 2014, [Online]. Available: https://core.ac.uk/download/pdf/29409793.pdf%0Ahttps://dspace.lib.cranfield.ac.uk/handle/1826/9244
- [18] D. P. Raymer, "Aircraft Design: A Conceptual Approach," 1989. [Online]. Available: https://api.semanticscholar.org/CorpusID:109869727